

## A Compact Triple-Band Antenna with Dual-Polarization Characteristics

Ting Wu\*, Hao Bai, and Xi-Zheng Ke

**Abstract**—A novel and compact triple-band Y-shaped monopole antenna with dual-polarization characteristics is proposed. The antenna is composed of a partial ground and a microstrip-fed radiating patch that consists of two unequal monopole arms and a circle monopole. The antenna is able to generate three separate impedance bandwidths of 230 MHz (2.30–2.53 GHz), 170 MHz (3.38–3.55 GHz), and 4170 MHz (4.35–8.52 GHz), which can cover both of the WLAN bands (2.4 and 5.8 GHz) and WiMAX band (3.5 GHz). By utilizing different lengths of monopoles, two circularly polarized bands at 2.4 GHz and 5.8 GHz are realized. Moreover, the antenna exhibits monopole-like radiation patterns and stable antenna gains across the operating bands. The effect of the antenna's key structural parameters on its performance was also analyzed.

### 1. INTRODUCTION

The rapid growth of modern wireless systems has increased the demand for compact antennas with multi-band resonance [1]. Recently, wireless local area network (WLAN) and worldwide interoperability for microwave access (WiMAX) have been widely used because they were recognized as a viable, cost-effective, and high-speed data connectivity solution [2]. In addition, for the wireless local area network (WLAN), circular polarization (CP) is often a good choice because of reduced multipath and antenna orientation constraints. Also CP antennas operate better in dreadful weather and provide better mobility than linearly polarized antennas [3]. Thus, multiband linear and circular polarization performance is required in a single antenna [4].

To satisfy the multiband operation requirements, this type of antenna must be of a simple construction to make it cost-effective, compact in size, and easily integrated within the front-end circuitry of a transceiver [5]. As a good candidate, planar monopole antennas are regarded as good alternatives for wireless applications because some advantages such as omnidirectional radiation pattern, low profile and low cost. Therefore various types of monopole antennas have been proposed so far to satisfy the multiband operation requirements [6–9]. Numerous CP antennas have also been presented in recent years [10–12]. A miniaturized tri-band monopole antenna for WLAN/WiMAX applications is presented and investigated [13]. The proposed antenna is well designed and has good performance with simple structure. However these antennas can achieve either multiband or circular polarization, not both of them. In [1] and [5], the antennas were proposed to provide multiband with dual-polarization characteristics, however, both of them were dual-band, and only one CP band is achieved. Moreover, all of the antennas mentioned above are somewhat complicated in structure which limits their availability for practical applications.

In this letter, a relatively small tri-band microstrip-fed monopole antenna is presented for WLAN and WiMAX applications. With two unequal monopole arms and a circle monopole, the antenna provides three wideband impedance bandwidths of 230 MHz, 170 MHz, and 4170 MHz with

---

Received 22 March 2017, Accepted 3 May 2017, Scheduled 27 June 2017

\* Corresponding author: Ting Wu (wutingzdh@xaut.edu.cn).

The authors are with the Xi'an University of Technology, Xi'an, Shaanxi 710048, People's Republic of China.

corresponding frequency bands of 2.30–2.53 GHz, 3.38–3.55 GHz, and 4.35–8.52 GHz, respectively. By utilizing different lengths of monopoles, two circularly polarized bands at 2.4 GHz and 5.8 GHz are realized. In addition, the antenna shows monopole-like radiation patterns and stable antenna gains across the operating bands. Moreover, the proposed antenna is extremely simple. Detailed geometry configuration and experimental results of the proposed antenna are demonstrated in the following parts.

## 2. ANTENNA DESIGN AND ANALYSIS

### 2.1. Antenna Design and Evolution

The configuration and photograph of the proposed antenna are shown in Figure 1 and Figure 2, respectively. The antenna is designed on an Arlon AD255A substrate with a relative dielectric constant of 2.55, loss tangent of 0.0015, and thickness of 1.5 mm. The overall dimension of the antenna is only  $35 \times 45 \text{ mm}^2$ . It is simply composed of a partial ground and a microstrip-fed printed Y-shaped radiating patch that consists of two unequal monopole arms and a modified circle. The two arms are deformed into L shape to save space and the middle circle monopole is embedded in the Y-shaped monopole. The dimension of the proposed antenna is chosen to be  $L1 = 35 \text{ mm}$ ,  $L2 = 13 \text{ mm}$ ,  $L3 = 6.8 \text{ mm}$ ,  $L4 = 12.4 \text{ mm}$ ,  $L5 = 8.8 \text{ mm}$ ,  $L6 = 18.4 \text{ mm}$ ,  $L7 = 8 \text{ mm}$ ,  $L8 = 5.2 \text{ mm}$ ,  $L9 = 6.5 \text{ mm}$ ,  $W1 = 45 \text{ mm}$ ,  $W2 = 2.4 \text{ mm}$ ,  $W3 = 11 \text{ mm}$ ,  $H = 1.6 \text{ mm}$ ,  $R1 = 5.5 \text{ mm}$ . The electromagnetic software Ansoft HFSS 13.0 is employed to perform the design.

The evolution of the proposed triple-band antenna design is presented in Figure 3 to explain the process of antenna design. And its corresponding simulated reflection coefficient ( $S_{11}$ ) is shown in Figure 4. First, a microstrip-fed Y-shaped radiating patch that consists of two unequal monopole arms

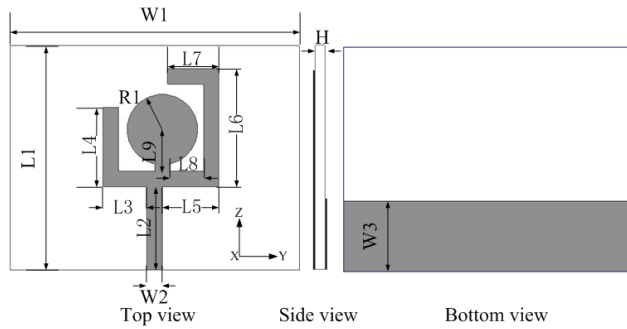


**Figure 1.** Configuration of the proposed antenna.



**Figure 2.** Photograph of the proposed antenna.

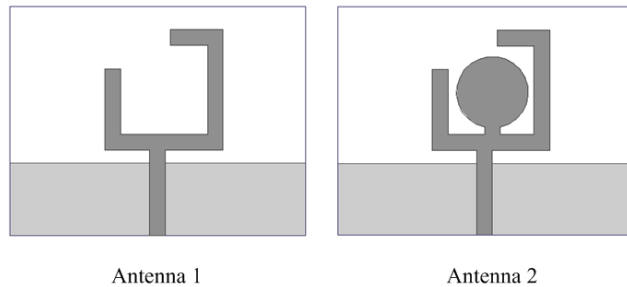


**Figure 3.** Geometry of various antennas involved in the design evolution process.

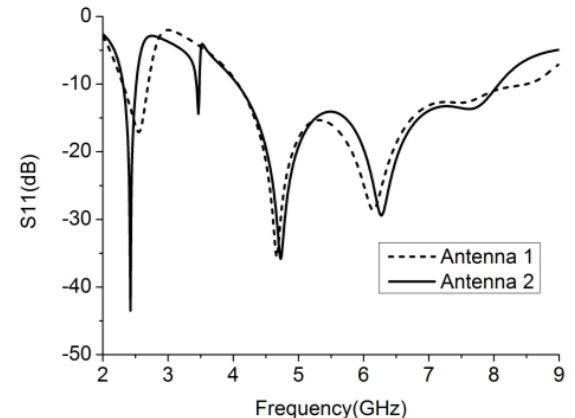


**Figure 4.** Simulated  $S_{11}$  of various antennas.

with a partial ground is designed. This simple design can obtain two resonant frequency bands as shown in Figure 4, ranging from 2.3–2.5 GHz and 4.5–8.5 GHz, which satisfies the lower and upper WLAN bands respectively. After that, a circle monopole is embedded in the Y-shaped monopole to generate an operation band at 3.5 GHz. The length of the circle monopole is approximately one quarter resonant wavelength. Thus, LP band is formed. So antenna 2 (the proposed antenna) can generate three distinct operation bands.

## 2.2. The Analysis of Circular Polarization

As for circular polarization characteristic, we make use of different monopole lengths to provide the  $90^\circ$  phase difference. By utilizing two different lengths of monopoles, we realize a change in the electric current phases of the monopoles. Basically, the radiated field is the superposition of radiation of monopoles currents. There are two orthogonal resonant paths formed by the monopoles. One path is formed by the two unequal monopole arms while another one is formed by the left monopole arm and the middle monopole. The length of the left monopole arm is  $L_{P1} = 32.2$  mm ( $L2 + L3 + L4$ ), the right one  $L_{P2} = 48.2$  mm ( $L2 + L5 + L6 + L7$ ), and the middle one  $L_{P3} = 25.2$  mm ( $L2 + L5 - L8 + L9 + R1 - W2$ ). The path  $L_{P1}$  is  $0.40\lambda_g$  at the resonant frequency of 2.4 GHz, and  $L_{P2}$  is  $0.63\lambda_g$ .  $L_{P1}$  is approximately  $\lambda_g/4$  shorter than the  $L_{P2}$ .  $\lambda_g$  is the dielectric wavelength and can be calculated by the following equation:

$$\lambda_g = \frac{\lambda_0}{\sqrt{\epsilon_{eff}}} \quad (1)$$

where  $\lambda_0$  is the air wavelength, and  $\epsilon_{eff}$  is the effective dielectric constant. So the left monopole arm generates a wave with relative phase advance, whereas the right one generates a wave with relative phase delay. Taking advantage of this lead and lag phases, the phase difference of  $90^\circ$  is tuned and a CP operation band (2.34–2.45 GHz) is achieved. In the same way, another embedded CP operation band (5.75–6.15 GHz) is achieved by the resonant path composed of the left monopole arm and middle monopole. Therefore, the proposed antenna provides a circularly polarized band at 2.4 GHz and an embedded circularly polarized band at 5.8 GHz. To deeply and clearly explain CP mechanism, the

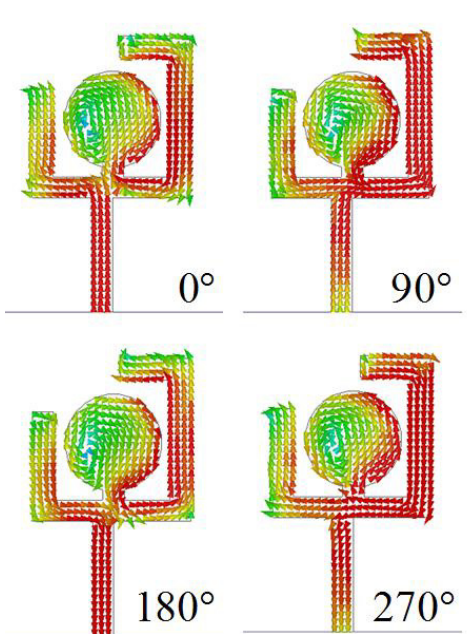


**Figure 5.** Simulated surface current distribution of the antenna at 2.4 GHz in  $0^\circ$ ,  $90^\circ$ ,  $180^\circ$ , and  $270^\circ$  phase.

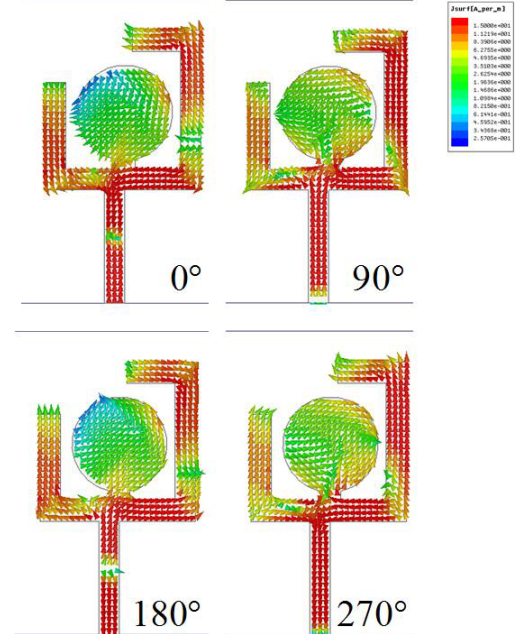


**Figure 6.** Simulated surface current distribution of the antenna at 5.8 GHz in  $0^\circ$ ,  $90^\circ$ ,  $180^\circ$ , and  $270^\circ$  phase.

simulated surface current distributions at 2.4 GHz and 5.8 GHz as the phase changes from  $0^\circ$  through  $270^\circ$  degrees are illustrated in Figure 5 and Figure 6, respectively. Changes in the electric current phases of the monopoles are realized by utilizing two different lengths. There will be right hand circular polarization.

### 3. RESULTS AND DISCUSSION

The simulated and measured reflection coefficients ( $S_{11}$ ) against the frequency of the proposed antenna are illustrated in Figure 7. The measured 10-dB impedance bandwidth for the three frequency bands are 230 MHz (2.30–2.53 GHz), 170 MHz (3.38–3.55 GHz), and 4170 MHz (4.35–8.52 GHz) respectively. Figure 8 illustrates the AR spectrums. We can see clearly that the measured 3-dB AR bandwidths are approximately 110 MHz (2.34–2.45 GHz) and 400 MHz (5.75–6.15 GHz). It is observed that both CP bands are completely inside their respective impedance bands. Hence, the antenna provides circular polarization performance covering the lower and upper WLAN bands and linear polarization performance covering WiMAX band. Good agreement is obtained between simulation and measurement with an acceptable frequency discrepancy.

In order to investigate the effects of various parameters on the resonant frequency of the antenna, parametric studies have been carried out. The simulated  $S_{11}$  curves and AR curves for different lengths of the right monopole arm  $L7$  are shown in Figure 9 and Figure 10 respectively. It can be seen that increasing of the length of the right monopole arm will lower the center frequency of the first impedance

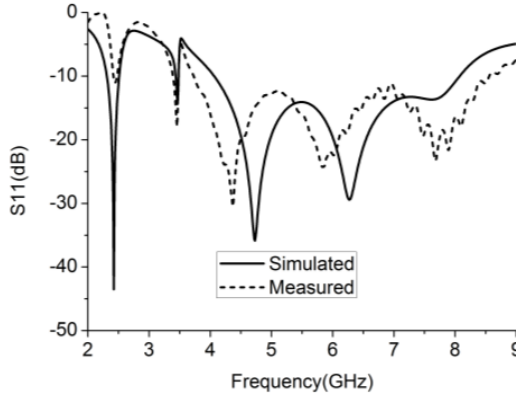


Figure 7. Measured and simulated  $S_{11}$  of the proposed antenna.

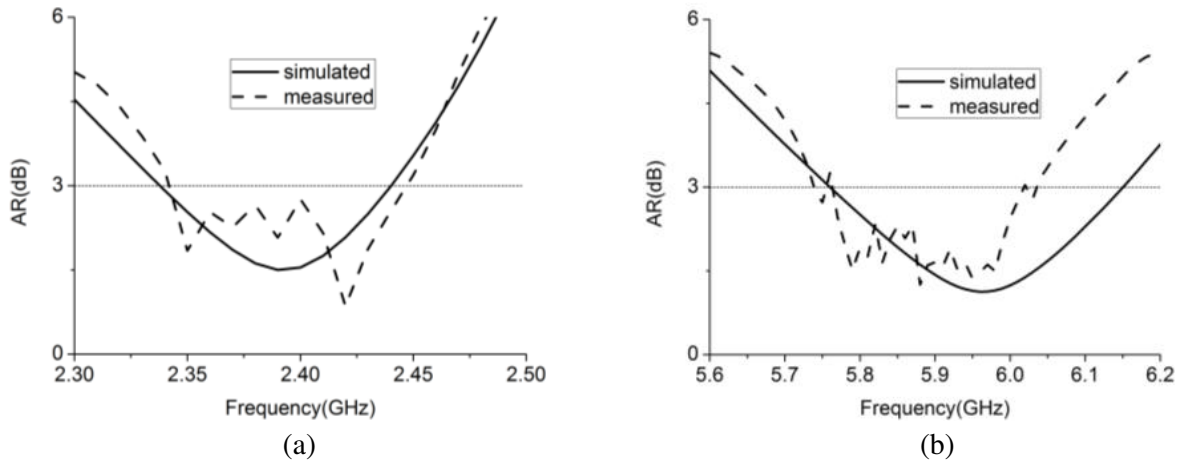
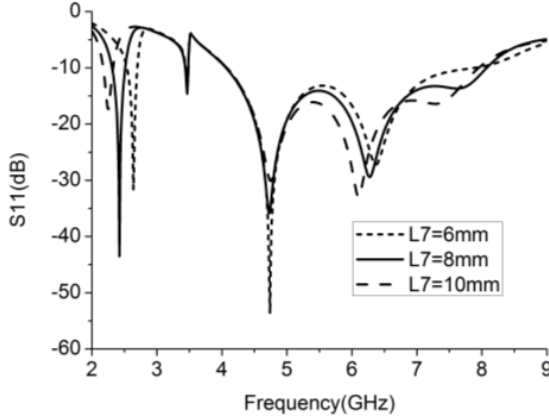
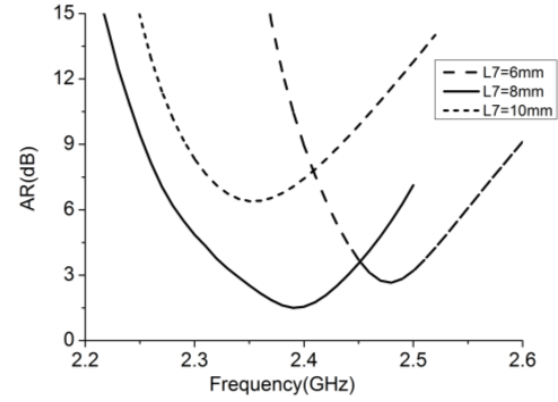


Figure 8. Simulated and measured axial ratio of the proposed antenna. (a) 2.4 GHz, (b) 5.8 GHz.

band while the other two bands nearly unchanged. And the center frequency of the first AR band becomes lower with  $L7$  increasing. Figure 11 shows the simulated  $S_{11}$  curves for different radius of the middle circle monopole  $R1$ . As shown in this figure, the center frequency of the middle band will shift



**Figure 9.** Simulated  $S_{11}$  for different values of  $L7$ .



**Figure 10.** Simulated AR for different values of  $L7$ .

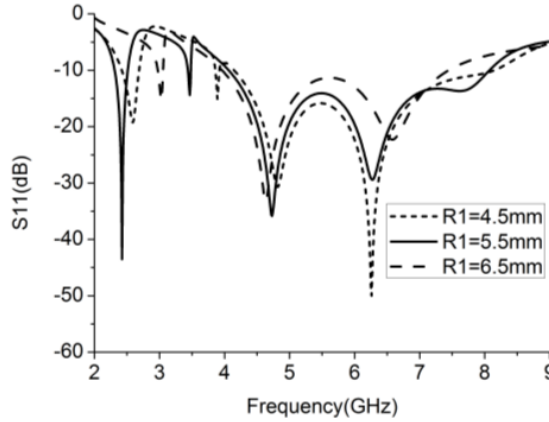


**Figure 11.** Simulated  $S_{11}$  for different values of  $R1$ .

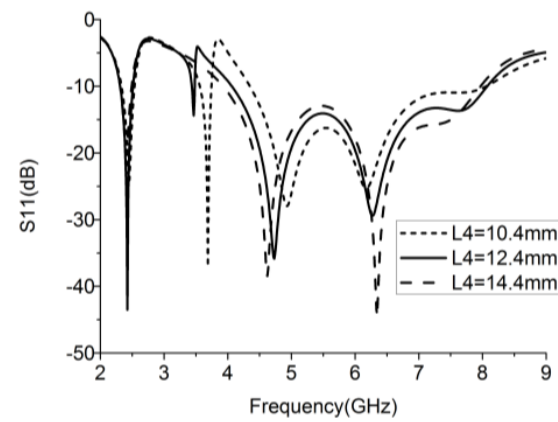


**Figure 12.** Simulated  $S_{11}$  for different values of  $L4$ .

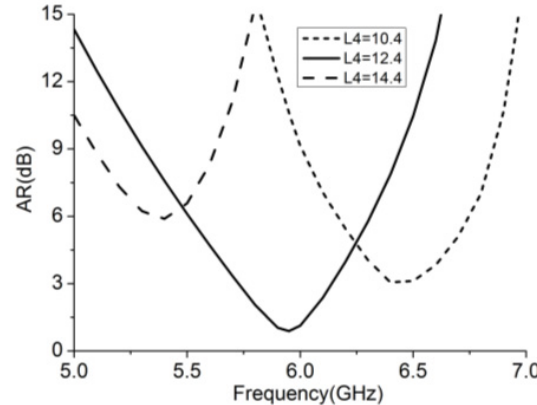


**Figure 13.** Simulated AR for different values of  $L4$ .

to lower frequency as the length of  $R1$  increases. The simulated  $S_{11}$  curves and AR curves for different lengths of the left monopole arm  $L4$  are shown in Figure 12 and Figure 13. It can be observed that as the  $L4$  elongated, the third band moves download. By taking advantage of these characteristics, changing of the lengths of the left, middle, and right monopoles can adjust the first, second, and third frequency bands accurately and easily.

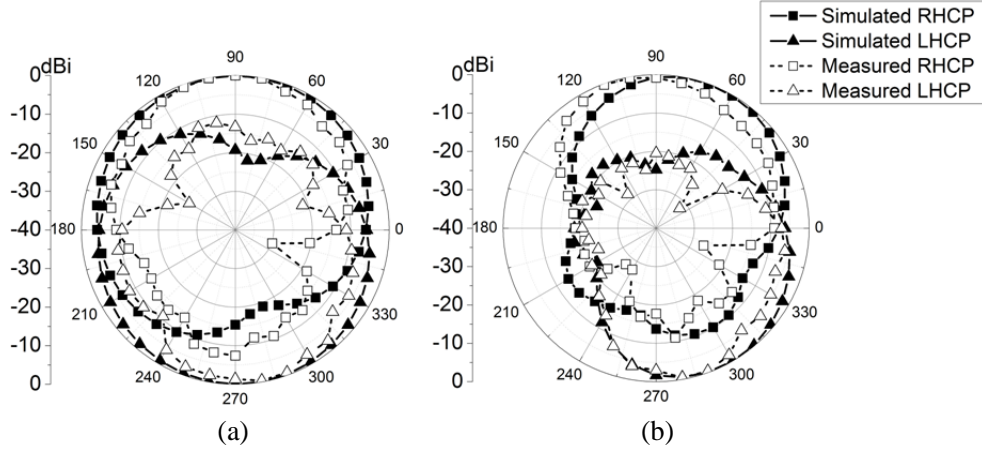


**Figure 14.** Measured and simulated radiation patterns for proposed antenna at different frequencies. (a) 2.4 GHz, (b) 5.8 GHz.

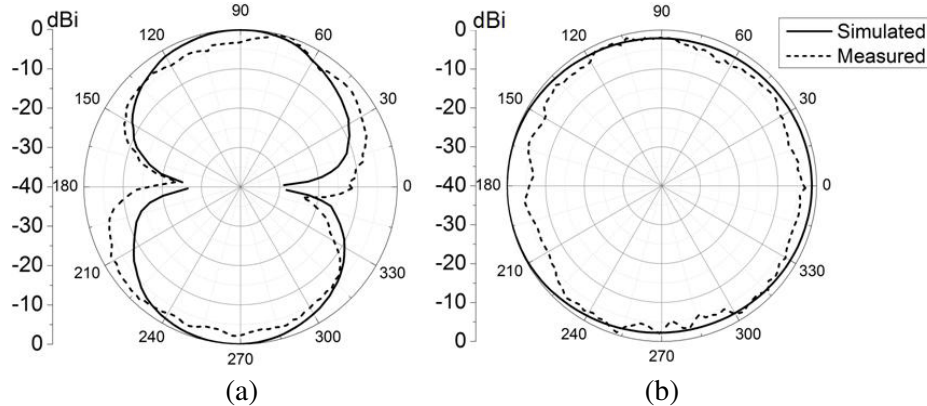


**Figure 15.** Measured and simulated radiation patterns for proposed antenna at 3.5 GHz. (a)  $E$ -plane, (b)  $H$ -plane.

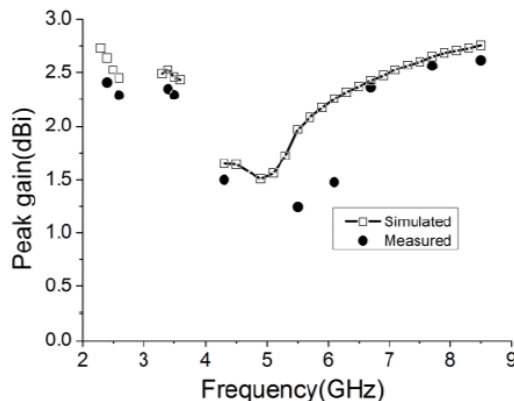


**Figure 16.** Measured gain of the proposed antenna.

The measured and simulated right-hand CP (RHCP) and left-hand CP (LHCP) radiation patterns at 2.4 GHz and 5.8 GHz are shown in Figure 14. We can see that both of the 2.4 GHz and 5.8 GHz bands are RHCP. And for the linearly polarized band, the measured radiation patterns in the *E*-plane and *H*-plane at 3.5 GHz is shown in Figure 15. From an overall view of these radiation patterns, the antenna behaves quite similarly to the typical printed monopoles at the frequency of 3.5 GHz. And at 2.4 GHz and 5.8 GHz, it can be seen that the antenna radiates an RHCP wave in the upper-half space. The gain of the proposed antenna for frequencies across the triple operating bands is stable and acceptable, as illustrated in Figure 16.

#### 4. CONCLUSION

A novel and compact tri-band microstrip-fed monopole antenna with dual-polarization characteristics is proposed. The proposed antenna can achieve circular polarization in two bands (2.34–2.45 GHz and 5.75–6.15 GHz) while linear polarization is in frequency band (3.38–3.55 GHz). The effect of varying the antenna's key parameters on its performance was also studied to acquire a deeper understanding and insight on the antenna. In addition, the proposed antenna has several other advantages such as small size, monopole-like radiation patterns, and stable antenna gains across the operating bands. These properties make the antenna suitable for multimode wireless communications systems in the WLAN, WiMAX applications.

#### REFERENCES

1. Thi, T. N., S. Trinh-Van, G. Kwon, and K. C. Hwang, "Single-feed triple-band circularly polarized spidron fractal slot antenna," *Progress In Electromagnetics Research*, Vol. 143, 207–221, 2013.
2. Li, X., Y. F. Wang, X. W. Shi, W. Hu, and L. Chen, "Compact triple-band antenna with rectangular ring for WLAN and WiMAX applications," *Microw. Opt. Technol. Lett.*, Vol. 54, No. 2, 286–289, 2012.
3. Rezaieh, S. A., "Dual band dual sense circularly polarized monopole antenna for GPS and WLAN applications," *Electron. Lett.*, Vol. 47, No. 22, 1212–1214, 2011.
4. Song, X., "Small CPW-fed triple band microstrip monopole antenna for WLAN applications," *Microw. Opt. Technol. Lett.*, Vol. 51, No. 3, 747–749, 2009.
5. Naser-Moghadasi, M., R. Sadeghzadeh, L. Asadpor, and B. S. Virdee, "A small dual-band CPW-fed monopole antenna for GSM and WLAN applications," *IEEE Antennas Wireless Propag. Lett.*, Vol. 12, 508–511, 2013.
6. Koley, S. and D. Mitra, "A planar microstrip-fed tri-band filtering antenna for WLAN/WiMAX applications," *Microw. Opt. Technol. Lett.*, Vol. 57, No. 1, 233–237, 2015.
7. Kang, L., X. H. Wang, H. Li, and X. W. Shi, "Planar monopole antenna with a compact radiator for tri-band applications" *Microw. Opt. Technol. Lett.*, Vol. 57, No. 3, 706–709, 2015.
8. Zhang, X. Q., Y. C. Jiao, and W. H. Wang, "Compact wide tri-band slot antenna for WLAN/WiMAX applications," *Electron. Lett.*, Vol. 48, No. 2, 64–65, 2012.
9. Zhu, J., M. A. Antoniades, and G. V. Eleftheriades, "A compact tri-band monopole antenna with single-cell metamaterial loading," *IEEE Trans. Antennas Propag.*, Vol. 58, No. 4, 1031–1038, 2010.
10. Chen, W.-F., D. Yu, and S.-X. Gong, "An omnidirectional triple-band circular patch antenna based on open elliptical-ring slots and the shorting vias," *Progress In Electromagnetics Research*, Vol. 150, 197–203, 2015.
11. Jou, C. F., J. W. Wu, and C. J. Wang, "Novel broadband monopole antenna with dual-band circular polarization," *IEEE Trans. Antennas Propag.*, Vol. 57, No. 4, 1027–1034, 2009.
12. Chen, C. and E. K. N. Yung, "Dual-band dual-sense circularly-polarized CPW-fed slot antenna with two spiral slots loaded," *IEEE Trans. Antennas Propag.*, Vol. 57, No. 6, 1829–1833, 2009.
13. Huang, S. S., J. Li, and J. Z. Zhao, "Design of a compact triple-band monopole planar antenna for WLAN/WiMAX applications," *Progress In Electromagnetics Research C*, Vol. 48, 29–35, 2014.